RSC Advances

PAPER

Cite this: *RSC Adv.*, 2015, **5**, 30023

Elucidation of acid strength effect on ibuprofen adsorption and release by aluminated mesoporous silica nanoparticles†

N. H. N. Kamarudin,[a] A. A. Jalil,*[ab] S. Triwahyono,[cd] M. R. Sazegar,[cd] S. Hamdan,[e] S. Baba[e] and A. Ahmad[ab]

Received 20th December 2014
Accepted 16th March 2015

DOI: 10.1039/c4ra16761a

www.rsc.org/advances

Mesoporous silica nanoparticles (MSN) with 1–10 wt% loading of aluminum (Al) were prepared and characterized by XRD, N_2 physisorption, ^{29}Si and ^{27}Al NMR, FT-IR and FT-IR preadsorbed pyridine. All samples were evaluated for ibuprofen adsorption and release. The results showed that MSN gave almost complete ibuprofen adsorption while the addition of 1, 5, and 10 wt% Al onto MSN (1Al-MSN, 5Al-MSN and 10Al-MSN) resulted in 35%, 58%, and 79% of adsorption, respectively. The characterization results elucidated that the highest adsorptivity of MSN was due to its highest surface silanol groups, while the increase in Brönsted acidity upon loading of Al provided more adsorption sites for the higher activity. Regardless of its highest adsorption capacity, MSN demonstrated the highest and fastest release (~100%) in 10 h, followed by 1Al-MSN, 5Al-MSN and 10Al-MSN. The increase in Al loading increased the acid sites that hold the ibuprofen molecules, which raised the retention in ibuprofen release. The pK_a of Si–OH–Al that is lower than Si–OH sites also attracted the ibuprofen more strongly, which resulted in the slower release of Al-MSN as compared to MSN. The cytotoxicity study exhibited that ibuprofen loaded Al-MSN was able to reduce the toxicity in the WRL-68 cells, verifying its ability to hold and slow the release of ibuprofen as well as minimize the risk of drug overdose.

1. Introduction

Drug delivery systems (DDS) are hybrid materials comprising a carrier and a drug that control the release rate of the biologically active molecules and reduce the limitations incurred with the classical administration of therapeutics, especially by minimizing the side effects.[1] The need for effective and patient-compliant drug delivery systems continuously leads researchers to design novel tools and materials. In recent years, mesoporous silica materials have been considered to be excellent candidates as carriers for drug delivery.[2,3] Mesoporous silicas such as MCM-41 and SBA-15 are solid materials comprised of a honeycomb-like porous structure with hundreds of empty channels (mesopores) that are able to absorb or encapsulate relatively large amounts of drugs or bioactive molecules. Their unique properties, such as good chemical and thermal stability, high surface area (>1000 $m^2\ g^{-1}$), large pore volume (>0.9 $cm^3\ g^{-1}$), tunable pore size with a narrow distribution (2–10 nm) make them potentially suitable for various controlled drug release applications.[4,5] The main advantage of ordered mesoporous silica as drug delivery vehicles is that one can either deposit or covalently bind active species to the inner surfaces or into the silica walls.[6] In addition, the high density of silanol groups can easily be functionalized with organosilanes, amines, or carboxyl groups, as well as inorganic groups such as metals and phosphonates in order to increase the drug delivery performances.[7] We have also reported the surface functionalization of mesoporous silica nanoparticles (MSN) using 3-aminopropyltriethoxysilane by co-condensation method to alter the silanol group coverage on the MSN surface, which then led to the differences in the mechanisms of ibuprofen loading and release.[8]

Mesoporous silicas incorporated transition metals and metal oxides are also known as potential materials for the adsorption of drugs. For instance, Cu^{2+} loaded onto SBA-15 was reported to be an effective adsorbent for naproxen *via* the metal–drug complexion,[9] while MnO-loaded SBA-15 performed well as a vehicle for a doxorubicin anti-cancer drug due to the accessibility of its paramagnetic center for encapsulation/

[a]*Department of Chemical Engineering, Faculty of Chemical Engineering, Universiti Teknologi Malaysia, 81310 UTM Johor Bahru, Johor, Malaysia. E-mail: aishah@cheme.utm.my*

[b]*Institute of Hydrogen Economy, Universiti Teknologi Malaysia, 81310 UTM Johor Bahru, Johor, Malaysia*

[c]*Department of Chemistry, Faculty of Science, Universiti Teknologi Malaysia, 81310 UTM Johor Bahru, Johor, Malaysia*

[d]*Ibnu Sina Institute for Fundamental Science Studies, Universiti Teknologi Malaysia, 81310 UTM Johor Bahru, Johor, Malaysia*

[e]*Department of Biological Science, Faculty of Bioscience and Bioengineering, Universiti Teknologi Malaysia, 81310 UTM Skudai, Johor, Malaysia*

† Electronic supplementary information (ESI) available. See DOI: 10.1039/c4ra16761a

sustained release/intracellular delivery of drugs.[10] On the other hand, zeolite was also reported as a good candidate drug carrier because the Al allows potential interactions with the drug. In a series of SiO_2/Al_2O_3 ratio studies, extra-framework Al in zeolite Y was found to form a complex with the drug 5-fluorouracil.[11] The Al content was also reported to generate acid sites that play an important role in ibuprofen adsorption.[12] However, the adsorptivity of such zeolites toward a wide range of drugs is still low due to their small pore sizes. In this sense, the use of larger pore size mesoporous silica with incorporated Al may offer greater advantages for drug adsorption. Besides, detailed reports on the understanding of acidity in terms of Lewis or Brönsted acid sites with relative to the drug delivery are still rare. Therefore, in this study 1–10 wt% Al was introduced to MSN and the physicochemical properties were studied by XRD, N_2 physisorption, ^{29}Si and ^{27}Al NMR, FT-IR and FT-IR of pre-adsorbed pyridine. The evaluation of Al-MSN was conducted on the adsorption and release of ibuprofen, a non-steroidal anti-inflammatory drug widely used in the treatment of pain and inflammation in rheumatic disease and other musculoskeletal disorders. Millions of kilograms of ibuprofen are produced and consumed annually by humans;[13] thus, the application of MSN to ibuprofen delivery is crucial and ever-continuing research.[14] We found that, apart from surface silanol groups, the strength of the Brönsted acidity also gave different interactions with ibuprofen which significantly affected its adsorption and release behavior. A cytotoxicity study of a selected sample was also conducted to show its potential in drug delivery system.

2. Experimental

2.1 Synthesis of MSN and Al-MSN

Mesoporous silica nanoparticle (MSN) was prepared by sol–gel method. 3.2 mmol of cetyltrimethylammonium bromide (CTAB, Merck Malaysia) surfactant was dissolved in 0.1 mol of distilled water, 0.2 mol of ethylene glycol (EG, Merck, Malaysia) as co-solvent, and 0.2 mol of 25% ammonia solution (NH_4OH, QRec Malaysia). After vigorous stirring for about 30 min with heating at 303 K, 1.2 mmol of tetraethyl orthosilicate (TEOS, MerckMalaysia) was added to the mixture to give a clear micelle solution. This white solution then stirred for another 2 h at 353 K and left aged for 24 hours. The precipitates of MSN were collected by centrifugation with 20 000 rpm for 10 min. The synthesized MSN was dried at 383 K and calcined at 823 K for 3 h to remove the surfactant. The material was denoted as MSN.

Al (1%, 5%, and 10% w/w) was loaded onto the MSN by the wet impregnation method. Aluminum nitrate ($Al(NO_3)_3$, QReC, Malaysia) solution was impregnated on MSN at 333 K, and was then dried in an oven at 383 K overnight before calcination in air at 823 K for 3 h. The aluminum-grafted MSN was denoted as MSN-Al_1, MSN-Al_5, and MSN-Al_{10} for 1%, 5%, and 10% Al loaded, respectively.

2.2 Characterization

The crystallinity of the catalysts was measured with a Bruker Advance D8 X-ray powder diffractometer (XRD) with Cu Kα (λ = 1.5418 Å) radiation as the diffracted monochromatic beam at 40 kV and 40 mA. ^{29}Si MAS NMR spectra were recorded on a Bruker Advance 400 MHz 9.4 T spectrometer at frequency of 104.2 MHz and 79.4 MHz, respectively. Nitrogen physisorption analysis was conducted with Brunnauer–Emmett–Teller (BET) method using a Micromeritics ASAP 2010 instrument. Fourier Transform-Infrared (Agilent Cary 640) was performed using the KBr method with a scan range of 400 to 4000 cm^{-1}. Before the measurement, the sample was evacuated at 573 K for 3 h. FT-IR spectra were recorded on a transmission spectrometer in which the sample was prepared as a self-supporting wafer and activated under vacuum at 673 K for 3 h in accordance with the previous report.[14–17] The adsorption of pyridine (2 Torr) was carried out at 423 K for 30 min, followed by outgassing at 423, 523 and 623 K for 30 min.[18]

2.3 Ibuprofen loading and release measurements

Powdered mesoporous samples were loaded with ibuprofen by soaking them in an ethanol solution of ibuprofen, followed by continuous stirring for 24 h at 310 K. A 1 : 1 (by weight) ratio of ibuprofen to solid sample was used. In practice, 150 mg of ibuprofen was dissolved in 5 mL of ethanol and 150 mg of dried mesoporous silica were added into this solution. Ibuprofen-loaded samples were recovered by filtration, washed with ethanol and dried for 24 h at 313 K. During the process, aliquots of 2 mL were withdrawn at pre-determined time intervals and centrifuged in a Hettich Zentrifugen Micro 120 before being analyzed by a UV-Vis spectrophotometer (Agilent Technologies) to determine the residual concentration of ibuprofen. Each set of experiments was performed three times. The adsorption band of ibuprofen was taken at a maximum wavelength (λ_{max}) of 264 nm.[19]

The ibuprofen release profile was obtained by adding 0.2 g of the drug-impregnated powders to a 200 mL round-bottom flask containing 100 mL of simulated body fluid (SBF) at 310 K under continuous stirring. The drug concentration in the release fluid at different release time points was determined using the UV-Vis spectrophotometer. In each case, 3 mL of the release fluid were taken out for analysis of the drug concentration, and then 3 mL of fresh SBF were added to the release system.

2.4 Cell culture

Human hepatic cells (WRL-68) obtained from American Tissue Culture Collection (ATCC) were cultured under standard conditions in a humidified 37 °C tissue culture incubator supplied with 5% CO_2 atmosphere, in Dulbecco's Modified Eagle's Essential Medium (DMEM) (Gibco-Invitrogen). The complete medium was supplemented with 1% (v/v) penicillin/streptomycin (10 000 units per mL each), 2% (v/v) L-glutamine (2 mM) and 10% (v/v) fetal bovine serum (FBS). The WRL-68 cells were harvested using trypsin (TrypLE, Gibco-Invitrogen) and seeded at 2×10^4 cells per mL in sterile 96-well plates prior to cytotoxic assay.

2.5 Proliferation test/MTT assay-cytotoxic test

Cytotoxic effects of MSN and Al-MSNs were tested on WRL-68 cells and determined by measuring the 3-(4,5-dimethylthiazol-2-yl)-2,5-diphenyltetrazolium bromide (MTT) dye metabolism. All the samples were dissolved in ethanol with serial dilution. Briefly, 2.0×10^4 cells were treated in triplicates with each type of samples. A total 10 μL MTT reagent (5.0 mg mL^{-1}) were added and cells incubated 4 hour in the dark at 37 °C. Isopropanol buffer were added to dissolve purple formazan precipitates and a microtiter plate reader (Research Instruments) was used to detect absorbance/reference at 570/650 nm.

3. Results and discussion

3.1 XRD analysis

Fig. 1 shows the XRD patterns of parent MSN and Al loaded MSNs with 1, 5, and 10 wt% Al. The small-angle XRD patterns exhibit a strong diffraction peak corresponding to (100) reflection and two smaller peaks assigned to (110) and (200) Bragg reflections. The diffraction of the samples occurred at $2\theta = 2.2°$, 3.9° and 4.5°, indicating well-ordered hexagonal arrays of mesopores.[20]

The characteristic hexagonal features of the parent MSN were maintained in all Al-MSN samples; however, there was a slight attenuation of peak intensity that was most likely due to a reduction in the X-ray scattering contrast between the MSN silica and the Al loaded MSN.[21] The Al loading onto the MSN decreased the peaks intensity, signifying the less ordered arrangement of the MSN framework.

3.2 N_2 physisorption analysis

Fig. S1† shows the nitrogen adsorption–desorption isotherms of bare MSN and the Al-MSNs. The surface area of the MSN was 1107 $m^2\ g^{-1}$, but the Al loading reduced the surface area to 916.8 $m^2\ g^{-1}$, 824.5 $m^2\ g^{-1}$, and 722.3 $m^2\ g^{-1}$ for 1Al-MSN, 5Al-MSN, and 10Al-MSN, respectively. It could be observed that all Al-MSN samples demonstrated a typical type IV isotherm with a remarkable decrease in nitrogen adsorption when compared to the parent MSN, suggesting cross-linking from calcination after the introduction of Al reduced the surface area.[22] The porosity of the samples was studied according to the pore size distributions depicted in the inset figures. All samples showed bimodal pore size distribution consisting of a primary pore at 3.65 nm and a secondary pore at 4.57 nm. The TEM images demonstrated in Fig. S2† show that the MSN and 10Al-MSN have almost similar particle sizes ranging from 60 to 80 nm.

3.3 NMR analysis

Solid state NMR has been widely used in elucidating the structure of mesoporous silica and zeolites, particularly for determination of coordination environment of ^{29}Si and ^{27}Al. Fig. 2A shows the Gaussian curve-fitting of ^{29}Si NMR spectra for 1Al-MSN and 10Al-MSN. Both samples consist of well resolved line at −102 to −112 ppm, which attributed to the formation of Q_3 and Q_4 species, and also a low intensity line in the range of −93 to −94 ppm, indicating the presence of Si in Q_2 environments.[23] It could be observed that the amount of Q_4 unit decreases by increasing Al loading in order to form more Q_3 and Q_2 species, indicating the possible isomorphous substitution of Al in the MSN framework.

The ^{27}Al NMR spectrum of 1Al-MSN and 10Al-MSN is depicted in Fig. 2B. The spectra show Al in two different coordination states at approximately 0 and 55 ppm, corresponding to octahedral (extra-framework Al) and tetrahedral Al coordination, respectively. It was observed from the 1Al-MSN spectrum that Al was incorporated mainly in tetrahedral coordination in the framework of MSN (Fig. 2B/a). However, the intensity of tetrahedral Al decreased when 10 wt% Al was loaded, in accordance with the emergence of octahedral Al.

The result suggests that when the Al content increases, it is deposited in the inner surface of the pores on the primary AlO_4 units leading to the formation of Al_xO_y, where the environment of the Al is octahedral.[24] The presence of extra-framework Al in this sample is also may be due to the existence of some Al sites

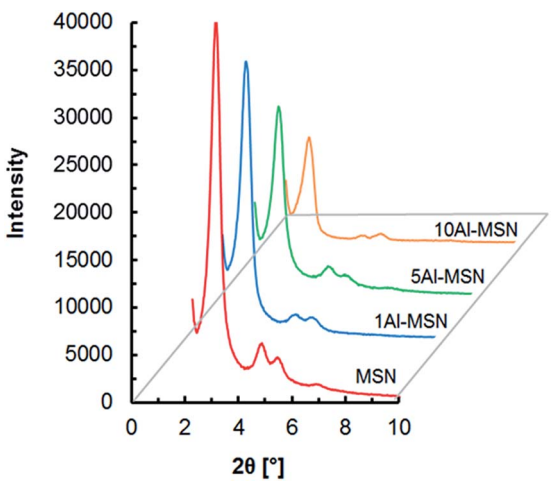

Fig. 1 X-ray diffraction pattern of bare MSN and Al-MSNs.

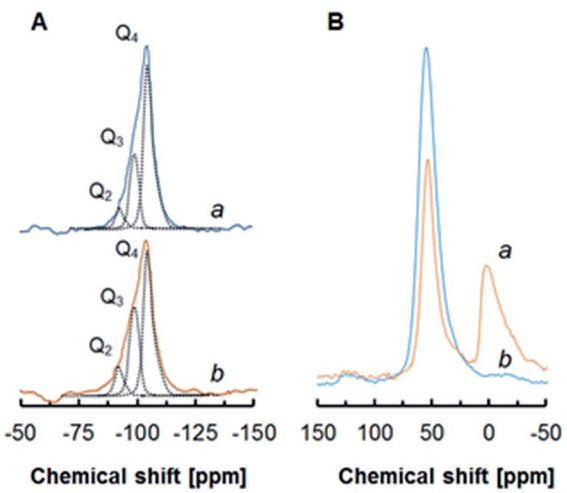

Fig. 2 (A) ^{29}Si NMR (B) ^{27}Al NMR of (a) 1Al-MSN (b) 10Al-MSN.

that are loaded outside of the structure and complete their coordination with water molecules or OH groups.[25] Relative to this observation, the existence of limiting factor for Al incorporation into MCM-41 framework is confirmed; due to the maximum amount of incorporated Al is limited by the number of available and accessible silanol groups.[26]

3.4 FT-IR analysis

Fig. S3A† illustrates the FT-IR spectra of all samples in the range of 2000–400 cm^{-1}. All Al-MSN samples exhibited bands attributed to water molecules retained by siliceous materials (1623 cm^{-1}), Si–O–(Al) vibrations in tetrahedral or alumino–oxygen bridges (1257 cm^{-1}), Si–O–Si asymmetric stretching (1064 and 1091 cm^{-1}), external Si–OH groups (933 cm^{-1}), Si–O–Si symmetric stretching (782 cm^{-1}), and Si–O–Si bending (466 cm^{-1}).[3,27] These results indicate the MSNs retained their siliceous structure despite the Al loading, demonstrating that no major changes occurred in the mesoporous framework. It is notable that the relative bands for MSN at 1623 cm^{-1}, 933 cm^{-1}, 782 cm^{-1} and 466 cm^{-1}, were reduced by Al loading, which may be due to the formation of the aluminosilicate (Si–O–Al) in the framework.

Next, the MSNs were evacuated at 673 K for 1 h prior to FTIR measurement to remove physisorbed water and the results are shown in Fig. S3B.† A sharp band was seen at 3737 cm^{-1} that was assigned to terminal silanol groups located on the external surface of the silica framework.[28] This band decreased markedly upon the Al loading, confirming the loading of Al on the surface of Si–OH groups to form acidic Si–(OH)–Al.[29]

This result supported the XRD data that demonstrated preservation of the uniform hexagonal framework of the MSN even after loading of Al up to 10 wt%. In addition, a broad and weak band was also detected at 3655 cm^{-1} (inset figure in Fig. S3B†), possibly associated with overlapping bands of weak acidic H-bonded vicinal silanol groups and Al–OH groups in extra-framework Al species.[30] These observations verified that incorporation of Al into the MSN framework is possible with the post-synthesis incorporation of Al, since it is introduced into the silica surface *via* a condensation process of the oxo–hydroxo species of Al with silicon species such as Si–(OH) terminal groups.[24]

The FTIR study was extended to observe the acidic character of all samples using pyridine pre-adsorbed FTIR spectroscopy and the results are shown in Fig. 3A. The bands at 1545 cm^{-1} and 1639 cm^{-1} were assigned to C–N stretching of pyridinium ions ($C_5H_5NH^+$) bound to Brönsted acid sites on the Al-MSN surface, while the bands at 1446 cm^{-1} and 1620 cm^{-1} were assigned to the vibration of physically adsorbed pyridine bound to Lewis acid sites. The band at 1596 cm^{-1} was assigned to H-bonded pyridine while the band at 1490 cm^{-1} was assigned to pyridine associated with both Brönsted and Lewis acids.

On purely siliceous MSN, pyridine forms hydrogen-bonded complexes with surface silanol groups, which are thus detected as Lewis acid sites.[31] In the case of Al-loaded MSN, increasing the amount of Al reduced the Lewis acid sites. Two main types of Lewis acid sites with were detected, moderate and strong, which is probably due to differences in the coordination number of surface Al atoms (tetrahedral and octahedral,

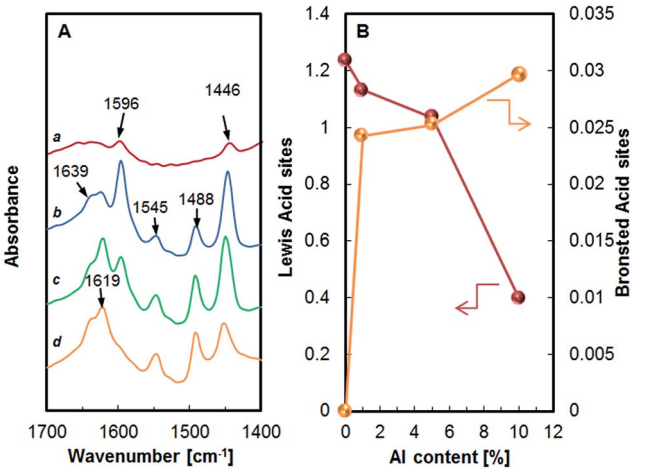

Fig. 3 (A) FT-IR preadsorbed pyridine spectra of (a) MSN; (b) 1Al-MSN; (c) 5Al-MSN; (d) 10Al-MSN outgassed in 423 K. (B) Relationship of Lewis acid sites and Brönsted acid sites with Al loading.

respectively) as a result of complex dehydroxylation processes involving the formation of Al–OH surface species and/or elimination of water molecules from the coordination sphere of Al^{3+} sites.[32]

Three signals at 1545 cm^{-1} and 1639 cm^{-1} were intensified with the addition of Al, suggesting the generation of Brönsted acid sites (Si–OH–Al) in the Al-MSNs.[33,34] For Al loaded MSN, the acidic sites generated by alumination could be the result of by either extra-framework Al species, such as AlO_5 and AlO_6, or defect sites such as AlO_3, or both.[35] A similar result was also reported for the incorporation of Al onto SBA-15, in which the Brönsted acid was generated in the aluminosilicate samples.[31] The formation of Brönsted and Lewis acid sites and their correspondence to the amount of Al grafted on the surface of the MSN is illustrated in Fig. 3B. As the Al content increased, a decrease in the number of Lewis acid sites was observed, since the increase in Al loading lowered the *d*-spacing, surface area, and pore volume and, consequently, reduced the number of acid sites accessible to the pyridine. This suggests that only a portion of the Al^{3+} was incorporated into the silica framework while the rest was likely present as extra-framework Al-rich species.[36]

Moreover, the amount of extra-framework Al increased, as indicated by NMR data; therefore, this also contributed to the reduced number of acid sites.[25] Simultaneously, the increase in Brönsted acid sites shows the increasing number of Si–OH–Al sites, which could also be expected to enhance the drug adsorption.

3.5 Adsorption of ibuprofen

The performance of all Al-MSNs with respect to ibuprofen adsorption was investigated and compared with the parent MSN (Fig. 4A). For the first 10 h, MSN demonstrated almost complete adsorption of ibuprofen, but the addition of Al onto the MSN reduced the adsorption capacity. Comparing all the Al-MSNs, 10Al-MSN displayed the highest adsorption (79%), followed by 5Al-MSN (58%) and 1Al-MSN (35%).

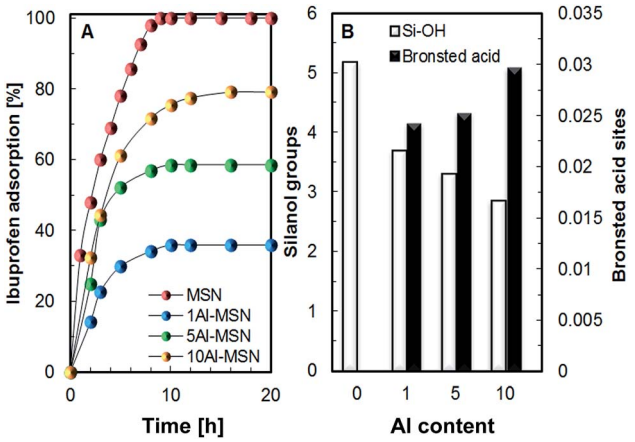

Fig. 4 (A) Ibuprofen adsorption for all samples. (B) Relationship of silanol group and Brönsted acid distribution with Al loading.

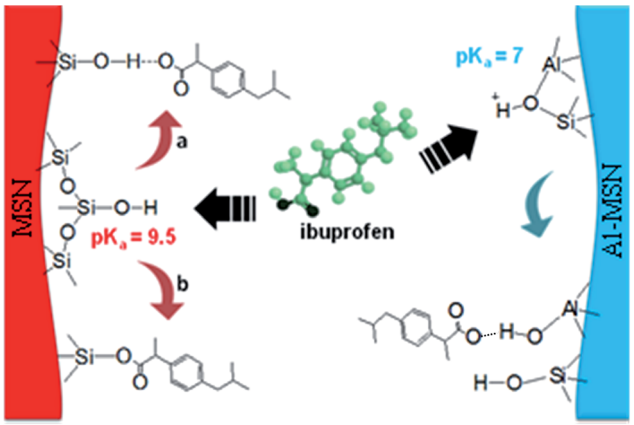

Fig. 5 Proposed mechanism of adsorption of ibuprofen on MSN and Al-MSN surface.

Previously, we reported that the driving force for the inclusion of ibuprofen inside the channels was the hydrogen bond interactions between the carboxyl groups of ibuprofen and the silanol groups on the surface of the MSN.[8] In contrast, herein the higher the Al loading, the higher the adsorptivity of the Al-MSNs toward ibuprofen. Despite the increasing pattern of adsorption with the Al loading percentage, the addition of 1% Al lead to a large difference of adsorption as compared to the bare MSN. This phenomenon was resulted from the formation of large amount of Lewis acid sites after the Al loading, which consists of the negatively charged AlO_4^- that resisted the ibuprofen adsorption. In accordance, the increase of Al loading gradually increases the Brönsted acid sites, Si–(OH)–Al which steadily enhances the ibuprofen loading.

In fact, from the NMR and FTIR results, the increasing Al content resulted in more isomorphous substitution occurring in the MSN framework, which simultaneously reduced the number of silanol groups. Thus, it could be the case that other factors in addition to silanol groups may play important roles in controlling the adsorption.

Fig. 4B shows the relationship between silanol groups and Brönsted acidity in terms of the Al content loaded onto the MSN. The numbers of silanol groups and Brönsted acid sites were determined from the absorbance of evacuated FTIR and pyridine pre-adsorbed FTIR data, respectively. The major contribution of silanol groups was revealed for the adsorption of ibuprofen onto parent MSN. However, the number of Brönsted acid sites increased proportionally with the increasing Al content onto the MSN, verifying the important role of Brönsted acidity in the adsorption of ibuprofen using Al-MSNs. Such organic molecules are supposed to have a strong tendency to be coordinated with Brönsted in preference to Lewis acid sites, which led to the higher adsorptivity. A similar observation was reported for the adsorption of organic compounds onto aluminosilica monoliths.[37] In addition, the evacuated FTIR data clarified that the location of the Brönsted acid sites was on the outer surface of the MSN framework, which considerably facilitated their accessibility to ibuprofen.[36]

The strength of the interaction between drugs and the silica surface is always variable and dependent on the adsorption active sites. It is well known that, at neutral pH, most of the ibuprofen was ionized and less was retained in the stationary phase.[13] In the case of acidic drugs that possess carboxylic groups (–COOH) such as ibuprofen, the interaction with silanol groups on MSN was postulated to occur by two different pathways as shown in Fig. 5. The first pathway is through hydrogen bonding of silanol groups with the hydroxyl groups of ibuprofen (Fig. 5a),[8,38] and the second is by way of ligand-exchange adsorption (Fig. 5b).[38]

Generally, the first pathway is favored to occur due to the lower demand of activation energy. Thus, both mechanisms may explain the higher adsorption capacity achieved by the parent MSN compared to the Al-MSNs. Based on the second mechanism, the proposed adsorption pathway when Al-MSNs are used is shown in Fig. 5, in which the anionic carboxyl groups of ibuprofen were attracted to the Brönsted acid sites of Si–$(OH)^+$–Al through an electrostatic interaction. A similar reaction pathway was reported for the interaction of methanol molecules with Brönsted acid sites, which occurred through the elimination of H_2O and bonding of CH_3 to the center O of Si–O–Al.[39] The results also suggest that the adsorption is not completely reversible. This phenomenon originates from the strong interactions between drugs and the silanol surface, as well as Brönsted acid sites, thus corresponding to irreversibly adsorbed drugs.

3.6 Release of ibuprofen

The dissolution tests from all ibuprofen-loaded MSNs were conducted in simulated body fluid dissolution medium at pH 7, and the results are presented in Fig. 6A. MSN showed the fastest and almost complete ibuprofen dissolution, despite its larger content of ibuprofen as compared to the three Al-MSNs. In contrast with the adsorption rate, the dissolution rate of ibuprofen was inversely proportional to the Al content loaded onto the MSN.

The highest ibuprofen release percentage was achieved when using 1Al-MSN (~100%), followed by 5Al-MSN (86%) and 10Al-

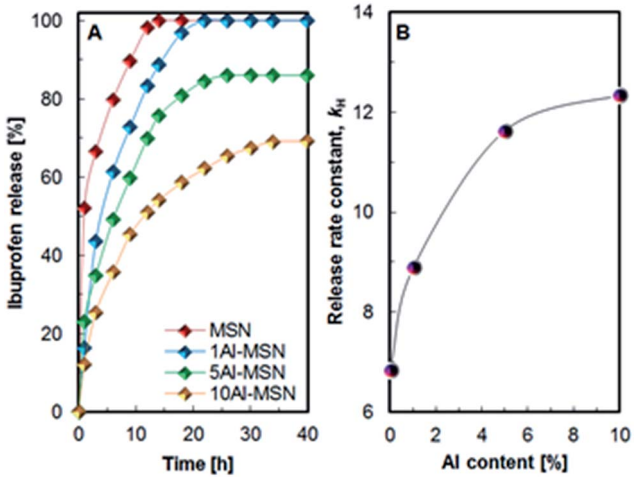

Fig. 6 (A) Ibuprofen release from all samples at 310 K and dissolution medium of pH 7.25. (B) Release rate constant of the Higuchi model (k_H) *versus* the number of Al content.

MSN (69%) after 15, 25, and 35 h of release time, respectively. The release of only 69% ibuprofen from 10Al-MSN suggested probable retention of ibuprofen due to the very strong interaction between the large amount of Si–(OH)–Al surface with the ibuprofen molecules.

According to the ibuprofen adsorption and release data, the Al content in the zeolite has a critical role in determining the drug loading and release profiles. Ibuprofen loading increased with increasing Al content for 1Al-MSN, 5Al-MSN, and 10Al-MSN, respectively. Different release behaviors also indicated that Al has an integral role in governing the interactions between Al-MSNs and ibuprofen. Due to the highest amount of silanol groups, the adsorption of ibuprofen onto MSN mostly occurs due to ibuprofen–silanol group interactions, which were clarified in a previous report.[8,40] However, as the Al loading increased, the number of silanol groups decreased even as, in contrast, the adsorption of ibuprofen increased. Apart from the MSN, the continuous loading of Al onto MSN resulted in the formation of Brönsted acid sites, which paralleled with the increase in ibuprofen adsorption. Thus, for all Al-MSN series, it is believed that the ibuprofen adsorption occurred through Si–(OH)–Al sites.

Based on the discussion in the previous section, it could be observed that the ibuprofen interacted with MSN and Al-MSN in different ways (Fig. 5). Based on the release pattern, MSN exhibited faster ibuprofen release compared to all Al-MSNs. It is speculated that this phenomenon is also due to the difference in OH group strength between Si–OH in MSN and Si–(OH)–Al in Al-MSN. The acidity of OH groups can be characterized in terms of the dissociation constant, pK_a, which has a value of 7.0 for the (A1–OH–Si) group and 9.5 for the Si–OH group.[41] This explains the retardation of ibuprofen release from Al-MSN, due to the stronger ibuprofen–Al-MSN interaction compared to the ibuprofen from MSN. A similar trend was observed in the case of ibuprofen interactions with zeolites with different silica to alumina ratios.[2] It was also reported that the ibuprofen was strongly coordinated to extra-framework Al (EFAL) resulting in reduced drug release. Zeolites with the highest Al content may interact with the ibuprofen species by hydrogen bonding of the carbonyl oxygen atoms with the zeolite's hydroxyl groups as well as through coordination between the drug molecules and Al atoms, specifically the extra-framework Al. In a different report, 5-fluororacil (5-FU) loaded on HY zeolites showed that HY with the greatest Al content exhibited less favorable release of 5-FU. In addition, previous literature has shown that 5-FU forms complexes with Al, such as binding of the 5-FU drug molecule through its –C═O and –N–H moieties with the Al^{3+} species.[42] As a consequence, Al-MSNs with the highest Al content may result in the formation of very strongly bound complexes in drug-loaded zeolite, thus limiting the release of the drug from the Al-MSN.

In order to investigate the mechanism of ibuprofen release from all Al-MSNs, the correlation of the kinetic curves was described by the Higuchi model, which is the first example of a mathematical model aimed at describing drug release from a matrix system (Fig. 6B). This model assumes that the systems are neither surface coated nor do their matrices undergo significant alteration in the presence of moisture.[43] According to this model, the release of species from pore voids is dependent on the square root of the length of time when delivery is based on a Fickian diffusion process. Pure diffusion is the rate-controlling release mechanism. Thus, the amount of ibuprofen released, Q_t per unit of exposed area at any time t can be described by the simple equation;

$$Q_t = k_H\sqrt{t} \quad (1)$$

where k_H is the release rate constant for the Higuchi model, which was obtained from the slope of the straight lines. This model fit well with the data on ibuprofen release, with correlation coefficients (R^2) of 0.9956, 0.9962, 0.9977, and 0.9985 for MSN, 1Al-MSN, 5Al-MSN and 10Al-MSN, respectively. The good linear fitting is indicative that release of the drug from the pores of the solids is basically a diffusive process.[44]

The initial burst of drug release was observed on all samples, which is explained by drug elution from the MSN surface. This was due to the high drug concentration gradient in the bulk solution–drug interface that can be attributed to loosely bound drug molecules on the outer silica walls.[45] The plot of the calculated k_H constants *versus* the Al content of the samples shows that the Higuchi constant increases as the acidic host–drug interaction becomes stronger, resulting in longer and slower release.

3.7 Cytotoxicity test

Nanoparticles are easily internalized into cells and some nanoparticles have even been shown to cross the blood brain barrier where they alter biological processes and cause toxicity.[46–48] Cell viability was determined by the MTT assay (activity of the mitochondrial respiratory chain). The MTT assay is based on the capability of viable cells to reduce the MTT tetrazolium salt (2-(4,5-dimethyl-2-thiazolyl)-3,5-diphenyl-2*H*-tetrazolium bromide) to produce insoluble purple-colored

formazan, which has to be dissolved subsequently in organic solvent for spectrophotometric dosage measurement.[49] In this study, the cytotoxicity of ibuprofen (IBU), 10Al-MSN, and ibuprofen-loaded 10Al-MSN (IBU–10Al-MSN) against the living cells was evaluated (Fig. 7A–C). The toxicity was determined through quantification of the proliferative capacity of adherent WRL-68 cells after 72 h of exposure tested with increasing concentrations of nanoparticles ranging from 0–8 mg mL^{-1}.

WRL-68 cells treated with different concentrations of sample showed significant differences from 10Al-MSN and IBU treated cells. The MSN-carrier suspension did not show fatal doses at IC_{50} compared to the IBU-treated suspension, which had an IC_{50} of 1 mg mL^{-1} and showed declining cell viability (48.83–2.88%) directly proportional to the increasing concentration of IBU (1–8 mg mL^{-1}) (Fig. 7D). In spite of this, the toxicity of the IBU suspension tested was significantly decreased when mixed with the 10Al-MSN. It was observed that the cell viability remained above 60% even at the maximum concentration tested at 8 mg mL^{-1} of 10Al-MSN and IBU–10Al-MSN. In fact, according to Fig. 4A, the ibuprofen contained in the 8 mg mL^{-1} 10Al-MSN was 6.32 mg. Thus, it is noteworthy that the IBU suspension was observed to cause high toxicity to the WRL-68 cells without being loaded in 10Al-MSN. Hence, the ibuprofen-loaded 10Al-MSN had showed lower toxicity, proving its ability to hold and slowly release the ibuprofen and reduces the risk of ibuprofen overdose toxicity.

4. Conclusion

The modification of the MSN by post-synthesis alumination had a significant effect on the adsorption and release of ibuprofen. Maximum ibuprofen adsorption was observed for the MSN, while the addition of Al resulted in reduction in its adsorption capacity to 35%, 58%, and 79% for 1Al-MSN, 5Al-MSN and 10Al-MSN, respectively. Due to the greater number of silanol groups in MSN, adsorption of ibuprofen mostly occurs due to the interaction between ibuprofen and silanol groups, as clarified in previous report. However, as the Al loading increased, the number of silanol groups decreased; yet, in contrast, adsorption of ibuprofen increased with increased Al loading. The increase in Brönsted acidity with Al loading provides more adsorption sites and this resulted to the higher activity. Regardless of possessing the highest adsorption capacity, MSN showed the fastest and greatest release in 10 h (~100%), followed, in order, by 1Al-MSN, 5Al-MSN and 10Al-MSN. Increasing the Al loading into the mesopore structure generated an increase in acid sites

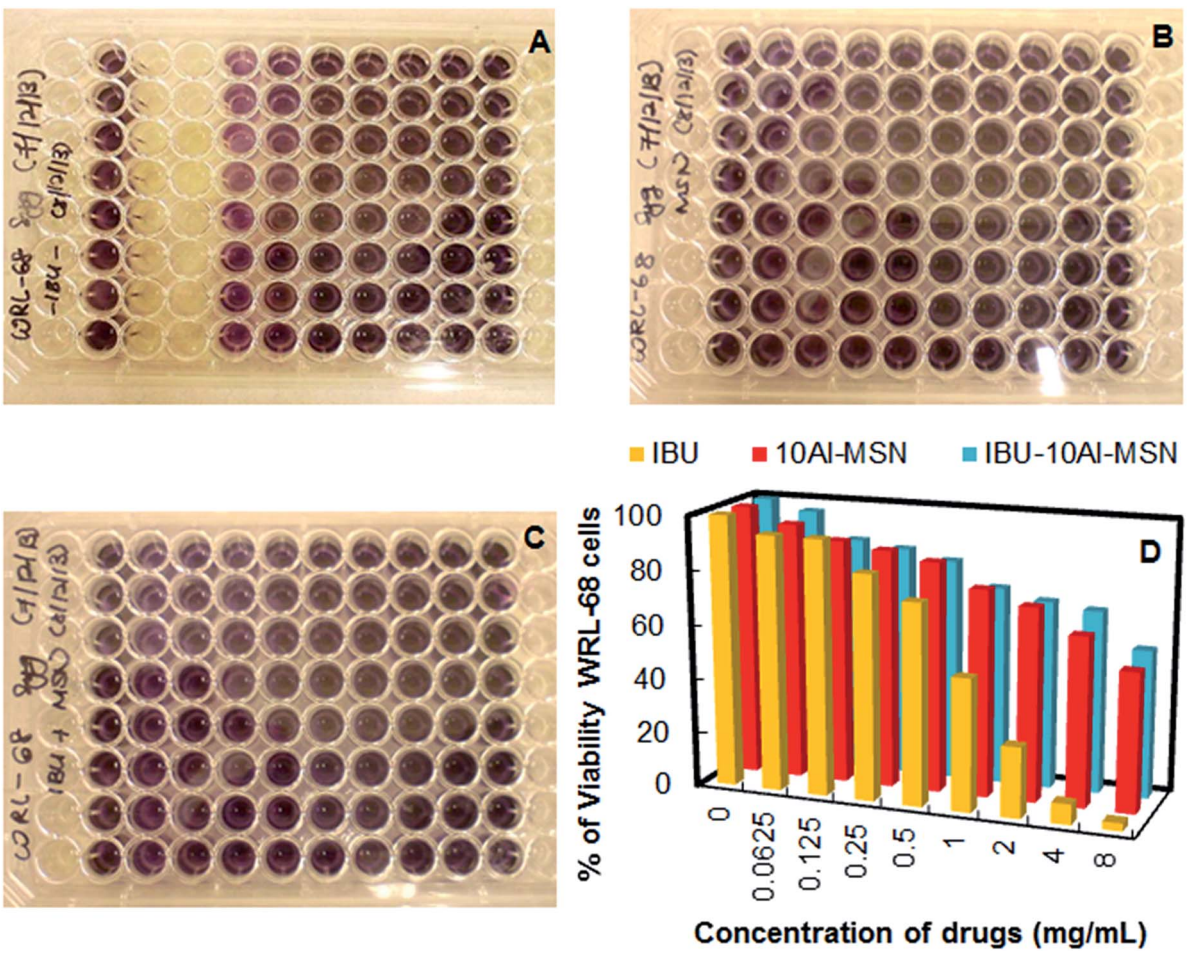

Fig. 7 (A) Ibuprofen; (B) 10Al-MSN; (C) IBU–10Al-MSN MTT viability assay; the solubilisation of insoluble purple-colored formazan MTT with isopropanol–HCl buffer; (D) cell viability of WRL-68 cells exposed to different concentrations of IBU, 10Al-MSN, and IBU–10Al-MSN.

but simultaneously decreased the well-defined hexagonal order and caused significant contraction of the pore diameter, which could retard ibuprofen release. It is also speculated that this phenomena is due to the difference in the strength of the OH group between the Si–OH in MSN and the Si–(OH)–Al in Al-MSN. From the cytotoxicity study, the ibuprofen suspension was observed to cause high toxicity to WRL-68 cells without being loaded in 10Al-MSN. The ibuprofen-loaded 10Al-MSN significantly reduced the toxicity, proving its ability to hold and slowly release the ibuprofen and minimize the risk of drug overdose.

Acknowledgements

The authors are grateful for the financial support by the Research University Grant from Universiti Teknologi Malaysia (Grant no. 02H76), the awards of My PhD Scholarship (Nur Hidayatul Nazirah Kamarudin) from Ministry of Higher Education, Malaysia, and to the Hitachi Scholarship Foundation for their support.

References

1 A. S. Hoffman, *J. Controlled Release*, 2008, **132**, 153.
2 P. Horcajada, C. Marquez-Alvarez, A. Ramila, J. Perez-Pariente and M. Vallet-Regi, *Solid State Sci.*, 2006, **8**, 1459.
3 Z. Tao, *RSC Adv.*, 2014, **4**, 18961.
4 I. Slowing, J. L. Vivero-Escoto, C.-W. Wu and V. S.-Y. Lin, *Adv. Drug Delivery Rev.*, 2008, **60**, 1278.
5 A. H. Karim, A. A. Jalil, S. Triwahyono, S. M. Sidik, N. H. N. Kamarudin, R. Jusoh, N. W. C. Jusoh and B. H. Hameed, *J. Colloid Interface Sci.*, 2012, **386**, 307.
6 R. M. Martín-Aranda and J. Cejka, *Top. Catal.*, 2010, **53**, 141.
7 S. K. Natarajan and S. Selvaraj, *RSC Adv.*, 2014, **4**, 14328.
8 N. H. N. Kamarudin, A. A. Jalil, S. Triwahyono, N. F. M. Salleh, A. H. Karim, R. R. Mukti, B. H. Hameed and A. Ahmad, *Microporous Mesoporous Mater.*, 2013, **180**, 235.
9 S. M. Rivera-Jiménez, S. Méndez-González and A. Hernández-Maldonado, *Microporous Mesoporous Mater.*, 2010, **132**, 470.
10 Y. Chen, H. Chen, S. Zhang, F. Chen, S. Sun, Q. He, M. Ma, X. Wang, H. Wu, L. Zhang, L. Zhang and J. Shi, *Biomaterials*, 2012, **33**, 2388.
11 A. Datt, E. A. Burns, N. A. Dhuna and S. C. Larsen, *Microporous Mesoporous Mater.*, 2013, **167**, 182.
12 S. K. Das, S. Kapoor, H. Yamada and A. J. Bhattacharyya, *Microporous Mesoporous Mater.*, 2009, **118**, 267.
13 T. Ahmad, B. Srihari, B. Alresheedi and N. M. Gowda, *Int. J. Pure Appl. Sci. Technol.*, 2012, **2**, 49.
14 A. A. Jalil, S. Triwahyono, M. R. Yaakob, Z. Z. A. Azmi, N. Sapawe, N. H. N. Kamarudin, H. D. Setiabudi, N. F. Jaafar, S. M. Sidik, S. H. Adam and B. H. Hameed, *Bioresour. Technol.*, 2012, **120**, 218.
15 M. R. Sazegar, A. A. Jalil, S. Triwahyono, R. R. Mukti, M. Aziz, M. A. A. Aziz, H. D. Setiabudi and N. H. N. Kamarudin, *Chem. Eng. J.*, 2014, **240**, 352.
16 M. A. Z. Abidin, A. A. Jalil, S. Triwahyono, S. H. Adam and N. H. N. Kamarudin, *Biochem. Eng. J.*, 2011, **54**, 124.
17 N. H. N. Kamarudin, A. A. Jalil, S. Triwahyono, R. R. Mukti, M. A. A. Aziz, H. D. Setiabudi, M. N. M. Muhid and H. Halimaton, *Appl. Catal., A*, 2012, **431–432**, 104.
18 H. D. Setiabudi, A. A. Jalil, S. Triwahyono, N. H. N. Kamarudin and R. Jusoh, *Chem. Eng. J.*, 2013, **217**, 300.
19 N. H. N. Kamarudin, A. A. Jalil, S. Triwahyono, V. Artika, N. F. M. Salleh, A. H. Karim, N. F. Jaafar, M. R. Sazegar, R. R. Mukti, B. H. Hameed and A. Johari, *J. Colloid Interface Sci.*, 2014, **421**, 6.
20 A. J. Di Pasqua, K. K. Sharma, Y.-L. Shi, B. B. Toms, W. Ouellettea, J. C. Dabrowiak and T. Asefa, *J. Inorg. Biochem.*, 2008, **102**, 1416.
21 I. J. Marques, P. D. Vaz, A. C. Fernandes and C. D. Nunes, *Microporous Mesoporous Mater.*, 2014, **183**, 192.
22 T. Yokoi, H. Yoshitake and T. Tatsumi, *Stud. Surf. Sci. Catal.*, 2004, **154**(A), 519.
23 P. Bhange, D. S. Bhange, S. Pradhan and V. Ramaswamy, *Appl. Catal., A*, 2011, **400**, 176.
24 M. Gomez-Cazalilla, J. M. Mérida-Robles, A. Gurbani, E. Rodriguez-Castellon and A. Jiménez-López, *J. Solid State Chem.*, 2007, **180**, 1130.
25 J. P. Lourenco, A. Fernandes, C. Henriques and M. F. Ribeiro, *Microporous Mesoporous Mater.*, 2006, **94**, 56.
26 R. Mokaya and W. Jones, *J. Mater. Chem.*, 1999, **9**, 555.
27 A. M. Klonkowski, T. Widernik, B. Grobelna, W. K. Jozwiak, H. Proga and E. Szubiakiewicz, *J. Sol-Gel Sci. Technol.*, 2001, **20**(2), 161.
28 N. W. C. Jusoh, A. A. Jalil, S. Triwahyono, H. D. Setiabudi, N. Sapawe, M. A. H. Satar, A. H. Karim, N. H. N. Kamarudin, R. Jusoh, N. F. Jaafar, N. Salamun and J. Efendi, *Appl. Catal., A*, 2013, **468**, 276.
29 K. Gora-Marek and J. Datka, *Appl. Catal., A*, 2006, **302**, 104.
30 J. M. R. Gallo, C. Bisio, G. Gatti, L. Marchese and H. O. Pastore, *Langmuir*, 2010, **26**, 5791.
31 A. A. Gurinov, Y. A. Rozhkova, A. Zukal, J. Cejka and I. G. Shenderovich, *Langmuir*, 2011, **27**, 12115.
32 G. Crepeau, V. Montouillout, A. Vimont, L. Mariey, T. Cseri and F. Maugé, *J. Phys. Chem. B*, 2006, **110**, 15172.
33 P. Kumar, N. Mal, Y. Oumi, K. Yamana and T. Sano, *J. Mater. Chem.*, 2001, **11**, 3285.
34 O. A. Anunziata, M. L. Martínez and M. G. Costa, *Mater. Lett.*, 2010, **64**, 545.
35 B. Dragoi, E. Dumitriu, C. Guimon and A. Auroux, *Microporous Mesoporous Mater.*, 2009, **121**, 7.
36 A. M. Venezia, R. Murania, V. La Parola, B. Pawelec and J. L. G. Fierro, *Appl. Catal., A*, 2010, **383**, 211.
37 S. A. El-Safty, M. Khairy and M. Ismael, *J. Environ. Anal. Toxicol.*, 2012, **2**(5), 147.
38 T. X. Bui and H. Choi, *J. Hazard. Mater.*, 2009, **168**, 602.
39 T. Blasco, *Chem. Soc. Rev.*, 2010, **39**, 4685.
40 J. Andersson, J. Rosenholm and M. Linden, in *Topics in Multifunctional Biomaterials and Devices e-book*, ed. N. Ashammakhi, 2008, vol. 1, pp. 1–19.

41 G. Sposito, *The chemistry of soils*, Oxford University Press, New York, 1989, p. 277.
42 K. K. Narang, V. P. Singh and D. Bhattacharya, *Polyhedron*, 1997, **16**, 2491.
43 S. Dash, P. N. Murthy, L. Nath and P. Chowdhury, *Acta Pol. Pharm.*, 2010, **67**(3), 217.
44 E. Aznar, F. Sancenón, M. D. Marcos, R. Martínez-Máñez, P. Stroeve, J. Cano and P. Amorós, *Langmuir*, 2012, **28**(5), 2986.
45 M. Bariana, M. S. Aw, M. Kurkuri and D. Losic, *Int. J. Pharm.*, 2013, **443**, 230.
46 B. M. Rothen-Rutishauser, S. Schurch, B. Haenni, N. Kapp and P. Gehr, *Environ. Sci. Technol.*, 2006, **40**, 4353.
47 C. M. Blumenfeld, B. F. Sadtler, G. E. Fernandez, L. Dara, C. Nguyen, F. Alonso-Valenteen, L. Medina-Kauwe, R. A. Moats, N. S. Lewis, R. H. Grubbs, H. B. Gray and K. Sorasaenee, *J. Inorg. Biochem.*, 2014, **140**, 39.
48 S.-J. Choi, J.-M. Oh and J.-H. Choy, *J. Inorg. Biochem.*, 2009, **103**, 463.
49 T. Mosmann, *J. Immunol. Methods*, 1983, **65**, 55.